Magnetic Resonance Letters xxx (xxxx) xxx

Contents lists available at ScienceDirect

Magnetic Resonance Letters

journal homepage: www.keaipublishing.com/MRL

The NMR core analyzing TOMograph: A multi-functional tool for non-destructive testing of building materials

Sabine Kruschwitz [a, b, *], Sarah Munsch [a], Melissa Telong [a], Wolfram Schmidt [a], Thilo Bintz [a], Matthias Fladt [a], Ludwig Stelzner [a]

[a] Bundesanstalt für Materialforschung und -prüfung, Unter den Eichen 87, Berlin, 12205, Germany
[b] Technische Universität Berlin, Gustav-Meyer-Allee 25, Berlin, 13355, Germany

ARTICLE INFO

Article history:
Received 15 December 2022
Received in revised form 28 February 2023
Accepted 9 March 2023
Available online xxx

Keywords:
Natural stone
Concrete
Sensitivity
Moisture transport
Cement hydration
Supplementary cementitious materials
Frost and salt attack
Fire spalling

ABSTRACT

NMR is becoming increasingly popular for the investigation of building materials as it is a non-invasive technology that does not require any sample preparation nor causes damage to the material. Depending on the specific application it can offer insights into properties like porosity and spatial saturation degree as well as pore structure. Moreover it enables the determination of moisture transport properties and the (re-)distribution of internal moisture into different reservoirs or chemical phases upon damage and curing. However, as yet most investigations were carried out using devices originally either designed for geophysical applications or the analysis of rather homogeneous small scale (< 10 mL) samples. This paper describes the capabilities of an NMR tomograph, which has been specifically optimized for the investigation of larger, heterogeneous building material samples (diameters of up to 72 mm, length of up to 700 mm) with a high flexibility due to interchangeable coils allowing for a high SNR and short echo times (50–80 μ s).

1. Introduction

Nuclear magnetic resonance (NMR) with focus on ^{1}H protons is increasingly applied for non-destructive testing applications of building materials. The quantification and localization of moisture as well as the analysis of its bonding state is crucial for investigating phenomena like hydration, transport and damage mechanisms within various building materials. The measurement principle is based on the alignment of the protons in a static magnetic field and their deflection by 90° using a radio frequency pulse, which oscillates with the Larmor frequency (causing the desired resonance effect). After the excitation, the protons relax back into the equilibrium state and two relaxation processes are measurable: the spin-spin (T_2) and the spin-lattice (T_1) relaxation [1–4].

As the measurable T_2 relaxation is influenced by the protons' bonding and their environment (pore size), it enables not only the determination of the moisture content/distribution [5,6] and the water-bearing pore sizes [7,8], but also the differentiation of various bonding types of hydrogen [9–11]. Thereby, the following relation exist: The stronger the bonding of the protons and the smaller the pore, the shorter becomes the relaxation time. Therefore, the measured signal, which is a sum

* Corresponding author. Bundesanstalt für Materialforschung und -prüfung, Unter den Eichen 87, Berlin, 12205, Germany.
E-mail address: sabine.kruschwitz@bam.de (S. Kruschwitz).

https://doi.org/10.1016/j.mrl.2023.03.004

of numerous exponentially decaying signals, has to be converted into a T_2 relaxation time distribution by the use of a numerical inversion.

For the purposes named above, there are numerous specific requests to the NMR device. On the one hand, it is necessary to be able to have a dead time (echo time) as short as possible, but on the other hand, the sample sizes should be at least large enough to be representative in terms of e.g., existing aggregates.

However, so far mostly devices from the geophysics sector have been used which were originally built for the exploration of oil deposits or aquifer properties [1,12]. Other working groups have used different types of the NMR-MOUSE, which allows single-sided access to also larger samples but feature limited penetration depth and, hence, a lower signal-to-noise ratio. Devices such as the Rock Core Analyzer [7,13] work with a homogeneous magnetic field and enable measurements with higher signal-to-noise ratios (SNR), but with limited sample sizes. However, these were mainly built for zero-dimensional (0D) measurements and did not allow CPMG measurements of thin slices using short echo times. Additionally, the SNR is limited by the relatively low operating frequency of 2 MHz. An increase of the frequency will lead to higher SNR [14].

Fig. 1 Since April 2019, the authors of this article are working with an NMR tomograph from Pure Devices GmbH, which was particularly optimized for the investigation of building materials. The device was constructed for a maximum sample diameter of 72 mm and length of up to 800 mm [15,16]. It operates at a frequency of 8.9 MHz and the resolution, the echo time, the SNR and the measurement type can be adjusted by means of exchangeable coils. Depending on the coil size and type used, the minimum echo time varies between 50 μs and 80 μs. Short echo times are especially relevant for the detection of hydrogen protons, which are either chemically bound into the sample's matrix or strongly bound to the pore surface (as for example in very small or partially saturated pores).

The tomograph allows measurements along the entire sensitive length of the coils, as well as layer-selective and 2- or 3-dimensional measurements. A movable sample lifting system, as shown in Fig. 1 (right), guarantees the precise positioning of the sample. Table 1 summarizes the different setups and possible measurement configurations of the NMR tomograph depending on the different interchangeable coils. The slice coils enable both zero-dimensional (0D) and slice-selective measurements, whereas the image coils can also be used to perform 2D and 3D measurements as well as measurements of the whole sensitive volume (0D). The Combi coils are suitable for 0D, 1D and 2D measurements, and additionally, the smaller Combi coil can be used for 3D measurements.

2. Experimental

This paper reports on five actual but very diverse research topics, in which the NMR tomograph is currently used for building material characterization. The resulting signal data was analyzed using a software tool called nucleus [17]. This includes the inversion of the data into distributions of the transversal relaxation time (RTD).

2.1. Moisture content sensitivity

The accurate determination of moisture contents with NMR is a highly important task as the method is increasingly applied to building materials and consequently often during partial saturation. Besides application as the analysis of degradation phenomena and on-site measurements on cultural heritage [5,18,19], ^{1}H NMR is nowadays even used to monitor hydration processes in cementitious building materials [9,11,20]. Especially at these applications, the investigation material is often partially saturated and the precise determination of low moisture contents becomes highly relevant.

In the first research topic presented in this article, the focus lays on the sensitivity and the applicability of the NMR tomograph to samples containing low moisture contents. For this, we measured numerous samples from 19 sandstone types at different saturation states. Besides the full and partial saturation states, this also included oven-drying at 40 °C, 60 °C, 70 °C and 105 °C. To achieve partial saturation with low moisture contents, the samples were stored in dessicators with six varying saturated salt solutions until reaching mass consistency. The salt solutions thereby were needed to regulate relative

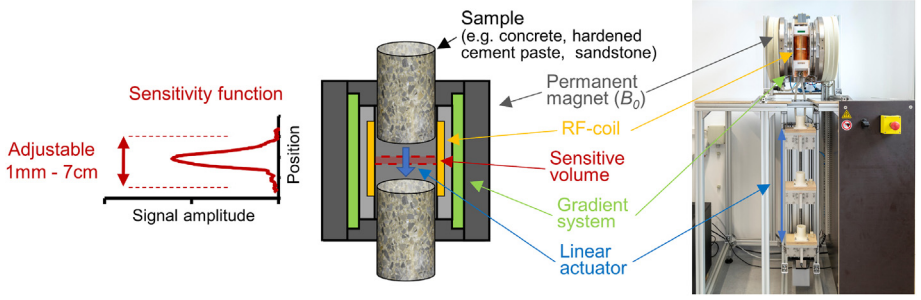

Fig. 1. Sketch of a slice-selective measurement (left) using the NMR tomograph with its movable lift system (right). See also Table 1.

Table 1
Various parameters of the changeable coils of the tomograph. The coil types are: S: Slice, I: Image, C: Combi.

Coil	22 I	32 I	32C	42 I	42 S	52 S	72 S	72C
Max sample diameter [mm]	22	32	32	42	42	52	72	72
Min echo time 0D [μs]	50	50	50	60	–	–	–	80
Min echo time 1D [μs]	50	50	50	60	60	70	80	80
Min echo time 3D [μs]	1800	1800	1800	1800	–	–	–	–
1D slice size [mm]	4–20	4–20	1–20	4–20	1–15	1–10	1–10	1–20

humidities ranging from 33% up to 96%. One group of samples was placed into a water bath and measured after 1 min, 15 min, 3 h and until reaching mass consistency. However, the maximum saturation was reached by first evacuating the samples with a vacuum pump and subsequently flooding with tap water. All samples had a cylindrical shape. The sample height thereby varied from 70 mm to 100 mm and the diameter from 19 mm to 22 mm.

The NMR measurements were conducted over the whole sensitivity length of the coil (no slice-selection) and with the minimum available echo time of 50 µs. Therefore, we used the two smallest available coils for maximum sample diameters of 22 mm and 32 mm. Gravimetrical weighing served as reference for the determination of the moisture content. For the monitoring of the sample weights at regular time intervals, we used a digital balance with a verification scale of 0.1 g and a readability of 0.01 g.

The results are shown in Fig. 2. Comparing the moisture contents determined from NMR measurements with the moisture contents obtained from gravimetrical weighing, it is striking that the fit line shows an offset (Fig. 2(a)). The moisture contents measured with NMR are slightly higher than those obtained from gravimetrical weighing. Even at theoretically dry samples (after oven-drying at 70 °C and 105 °C), a moisture content is measurable by use of NMR.

Following the norm [21], oven-drying at 70 °C serves as reference for the dry state of natural stone. Therefore, we subtracted the corresponding NMR signal of the dry samples from all NMR measurements. In this way, the moisture content determined with NMR after oven-drying at 70 °C was manually set to zero. Regarding Fig. 2(b), it can be seen, that the subtraction of the 70 °C NMR signal leads to an improvement of the fit and even the offset is reduced.

Finally, it can be summarized that the NMR tomograph with the technical composition used here has a high sensitivity and therefore enables the detection of (low) moisture contents down to around 0.03 g or 0.1 vol.-% in natural stone. The results show that even in oven-dried samples, a signal could be measured. In fact, this may (depending on the echo time used) originate from strongly bound hydrogen protons as e.g. physically bound to the pore wall or even within internal structures such as minerals. However, due to this phenomenon a correction of the measured signals is recommendable; especially when the results are compared to different methods and the dry state has to be defined uniformly.

2.2. Hydration process of alternative green building materials

As the global demand for cement-based building materials is dramatically increasing the production of classic Portland cement-based compositions results in high greenhouse gas emissions. Current efforts in building materials development are hence focused on reducing process related CO_2 emissions and maximizing the resource efficiency and circularity of the materials. Alternative green building materials contain so called supplementary cementitious materials (SCMs), which are mostly by-products from other industry sectors, to significantly reduce the amount of Ordinary Portland Cement (OPC) clinker, the main compound of our to-date cement mixtures. Consequently, studies regarding the hydration behavior and

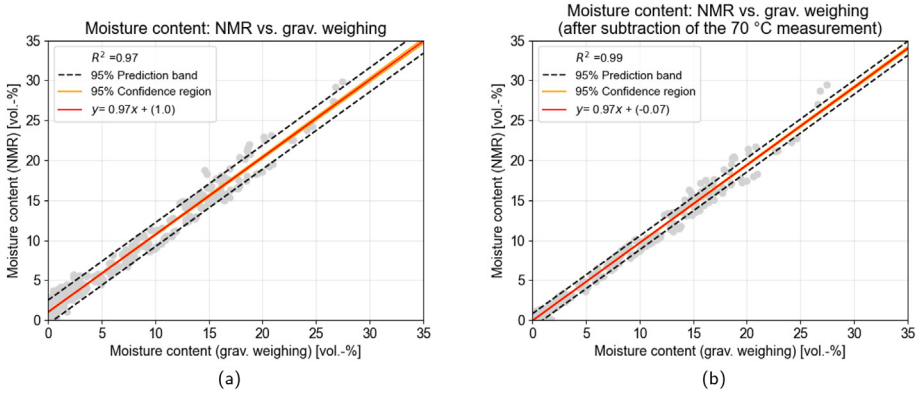

Fig. 2. Comparison of moisture contents in sandstone samples determined with NMR and gravimetrical weighing: (a) before subtraction of the 70 °C NMR measurement; (b) after subtraction of the 70 °C NMR measurement.

pore space characteristics of the new, yet to be optimized cement mixes containing different types and amounts of SCMs are needed.

A few working groups have tried to establish the NMR technique for the investigation of the reaction kinetics of cement-based samples and characterized the evolution of proton reservoirs (hydration products and pore spaces of different sizes) during hardening. Muller et al. [9], Ectors et al. [22], Jansen et al. [23] and Naber et al. [11] succeeded in attributing the evolution of the T_2 relaxation time of the different water populations throughout the hydration and compared their findings to results from X-ray diffraction (XRD) or scanning electron microscopy (SEM) analysis. These working groups, however, have focused on classic OPC based CEM I samples and have used very small sample volumes of only 5 mL, which enabled them to use very short echo times of only 5.2 μs.

The aim of our work now is to investigate the possibility of using the NMR tomograph allowing for much larger sample sizes of about 25 mL (which is favorable for inhomogeneous material such as cement especially when SCMs are added) while the lowest echo time in this setup is limited to 50 μs. For this experiment, we put fresh cement paste into 20 mm diameter glass tubes and seal them so that the total moisture content does not change. The samples are then measured for 40–100 h in 0D configuration using a 22 mm diameter coil and a CPMG pulse with an echo time of 50 μs at time intervals of 20–30 min.

The observed temporal changes in the measured T_2-relaxation time distributions (RTDs) are then attributed to the formation of the pore system in the fresh hardened cement paste and the changing amounts of free, physically and chemically bound water during hydration. We analyze the temporal change of the T_2 RTDs (currently) by analyzing the following three features:

1 Amplitude of the dominant mode in the RTD
2 T_2 log mean time of the RTD as defined in [24].
3 T_2 time of the dominant mode in the RTD

In Fig. 3 we compare these three features for a typical CEM I sample and a sister sample where 15% of the volume were replaced by rice husk ash (RSA), a pozzolanic supplementary cementitious material [25,26]. We use heat flow calorimetry (HFC) to study the hydration heat development. The general formation of hydration phases is for example described in Ref. [27]. Our data indicate that NMR feature 1 is a good indicator for the beginning of the accelerated C–S–H generation (i). The NMR features 2 and 3 coincide for the major part of the hydration for both mixes. However, we observe a clear divergence between them, which starts about when the mixtures pass from the plastic to the elastic state (ii) and probably becomes maximal during the second aluminate reaction peak (iii). Currently we interpret the convergence of the features as about the time when sulfate depletion in the mixes begins and C-A-H is formed (iv). It must be stated that the exact assignment of the characteristic times to certain phase formations (or dissolutions) are so far rather estimations, which have to be confirmed by further investigations such as XRD or SEM.

This example shows that we can achieve very similar results on significantly larger samples (25 mL vs 5 mL) and with significantly longer echo times (50 μs vs 5.2 μs). Furthermore, the joint evaluation of multiple NMR features seems promising

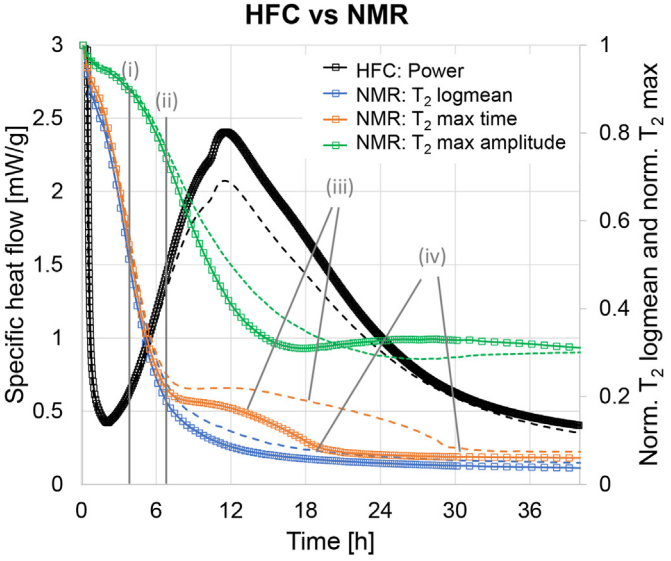

Fig. 3. HFC and NMR results obtained on CEM I (squares) and CEM I (square symbols) + 15% RSA (dashed lines) samples during the first 40 h of hydration. Four different states of hydration are marked with (i-iv).

for a deeper understanding of the complex hydration behavior of very likely more and more heterogeneous cement mixes involving significant amounts of SCMs or other types of recycled materials.

2.3. Ingress of moisture and deleterious ions

The transport of moisture and ions through building materials can have a major impact on the durability of these materials [28]. Their absorption can lead to chemical corrosion, physical degradation, or growth of microorganisms. Therefore, to estimate durability, it is important to understand how moisture and ions are transported.

Current testing methods have very low spatial resolution or are time consuming [28]. In addition, they often require the sample to be destroyed [29]. Moisture is usually measured only by weighing the samples [30]. Therefore, the transport of moisture and ions could only be considered separately. We have shown with a combined use of NMR and Laser-Induced Breakdown Spectroscopy (LIBS) that these transport mechanisms can also be studied in correlation. LIBS is a method that comes more and more into focus when it comes to measuring the ingress of ions such as chlorides, sulfates or nirates [31].

Capillary suction experiments were carried out on the specimens. A common ion that induces damage processes in building materials is chloride [32]. Therefore, two different solutions were prepared, one 1 mol/L and one 4 mol/L sodium chloride solution. This also served the purpose to investigate the influence of ion concentration on transport processes. For the capillary suction experiments, the samples were immersed 5 mm deep into the 10 mm high solutions after [30]. The suction experiments lasted between 3 and 300 h. Sample cylinders were removed from the solutions and measured first with the NMR tomograph, then with LIBS.

The progression of moisture within the samples was monitored using an NMR tomograph. LIBS was used to measure the ions. LIBS is a measuring system which heats the surface of the samples into a plasma using a high energy laser. The light emitted by the plasma has an element-specific spectrum, which can be analyzed by optical emission spectroscopy. In this way, a two-dimensional (2D) map can be created showing the elemental distributions on the sample surface [29,33]. To investigate the ion transport within the samples, these samples were sawed dry along the sample cylinder height.

Four different materials were tested, two sandstones, the Santa Fiora and the Skala and two cementitious building materials, a mortar and a concrete. The mortar was produced from Portland cement CEM I 42-R and standard sand up to a grain size of 2 mm. The concrete was made with the same cement and standard sand up to 8 mm grain size. All sample cores have a diameter of 40 mm and a height of 100 mm. At least 14 cylinders were made from each material. These were then dried in an oven at 70 °C and then laterally sealed with epoxy resin.

Two different types of measurements were used to investigate moisture transport, one-dimensional (1D) and three-dimensional (3D) measurements. For the 1D measurements, 2 mm thick slices were chosen, resulting in a moisture profile versus sample height. For the 1D measurements, the 42 Slice coil was used. The echo time was set to 0.06 ms.

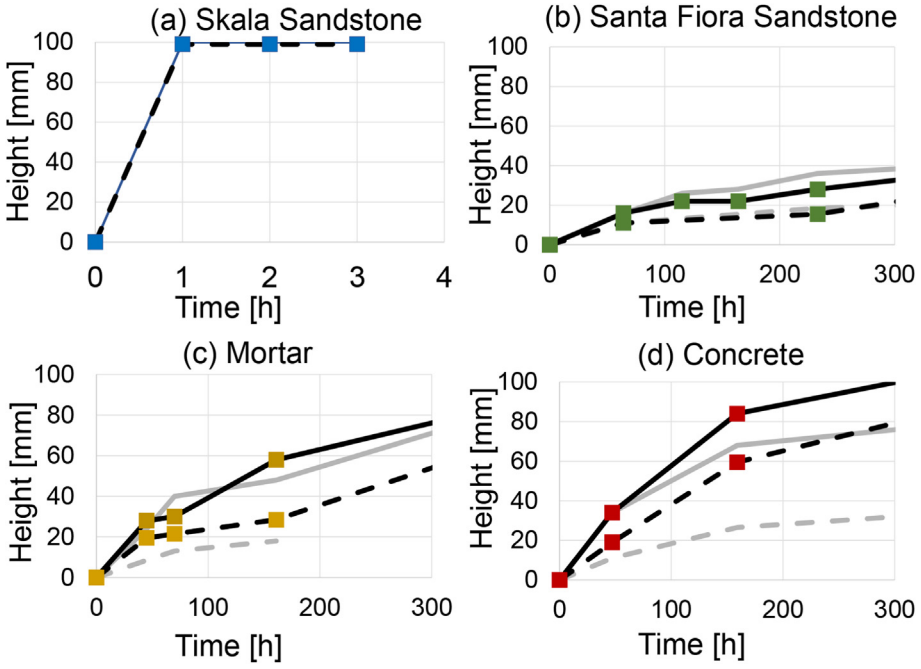

Fig. 4. Moisture and ion fronts in (a) Skala, (b) Santa Fiora, (c) mortar and (d) concrete. Moisture fronts have solid lines, chloride fronts have dashed lines. Graphs of the 1 mol/L suction experiments are more transparent, graphs of the 4 mol/L suction experiments have square symbols.

To better track transport through the materials, the penetration fronts were determined. They were defined as the height at which the signal fell halfway between the maximum and minimum. The moisture and ion fronts are shown in Fig. 4.

In general, the moisture always rises faster than the ions. In addition, the penetration height in the cementitious building materials, and therefore the penetration velocity, is directly dependent on the ion concentration. Moisture and ions in these materials seem to penetrate faster when the chloride concentration is higher. In this context, the sandstones appear to be less susceptible to changes in ion concentrations. In Skala, moisture and ions increase too rapidly to perceive differences, while Santa Fiora shows only minimally increased suction velocities at higher ion concentrations.

In addition to the 1D measurements, 3D measurements were made. Again, capillary suction experiments were performed for these measurements. However, the samples were not further investigated with LIBS, but were placed back into solution after measurement to continue the experiment.

For the 3D measurements, the measurement volume was divided into 1 mm $\times$ 1 mm x 1 mm volumes, called voxels. This creates a 3D image of the moisture distribution within the sample cylinders. The 42 Image coil was used for the 3D measurements. The echo time was set to 1.8 ms for the 3D measurements, since no useful results could be obtained with a lower time. The 3D measurements were performed only with the Santa Fiora sandstone, because with this material a water signal could be clearly distinguished from the noise despite the higher echo time.

To allow a comparison between 1D and 3D measurements, the signal of the 3D measurements was averaged to produce a profile as a function of height. As with the 1D measurements, the front of the moisture can then be determined. Fig. 5 shows the comparison between the 1D and 3D moisture fronts for the Santa Fiora Sandstone.

The moisture fronts of the 1D and 3D measurements are consistent, which shows that 1D as well as 3D measurements are suitable to follow the moisture progression through building materials. However, the higher echo time limits which materials can be used for such investigations, as it ensures that water signal and noise can not always be clearly separated.

2.4. Salt frost attack

Road pavement concretes in Northern and Central Europe usually have a high resistance to freeze-thaw with deicing salt due to the application of air entraining agents (AEA) to the concrete mixture. Adequately distributed micro air voids in the hardened concrete provide expansion space for freezing moisture and thus prevent cracks or surface scaling. A decrease of the resistance to salt frost attack has been discovered for internally hydrophobized road pavement concrete (IHRPC), which is originally intended to be used to increase the resistance to alkali aggregate reaction [34]. Although the distribution of air voids is modified by the hydrophobizing agent, the normative requirements e.g. spacing factor and micro air void content are fulfilled. Therefore, it seems counterintuitive that an internally hydrophobizing agent, protecting the concrete from external moisture penetration, causes increased surface scaling due to salt frost attack. The aim of the study is to investigate the moisture penetration behavior of treated with respect to untreated concrete samples exposed to freezing and thawing with deicing salt according to the Capillary suction of de-icing solution and freeze thaw (CDF) test [35]. With the NMR core analyzer, moisture profiles over the sample height of specially prepared core samples are acquired. Afterwards NMR amplitude vs. T_2-relaxation time distribution (RTD) provides qualitative information about a pore size-dependent moisture content for each NMR volume slice across the profile. Additionally, it may be possible to discriminate between potentially freezable and non-freezable moisture, since in a micro-to nanoporous material like cement paste an amount of moisture remains unfrozen even at - 20 °C [e.g. 36, 37, 38. However, it is important to notice, that at subfreezing temperatures unfrozen moisture from gel pores is dragged to concurrently forming ice lenses in larger capillary pores or air voids [39], causing shrinkage in the bulk cement paste and further expansion of ice lenses. We are not able to monitor this moisture redistribution while freezing, as we can only measure the moisture condition at 20 °C.

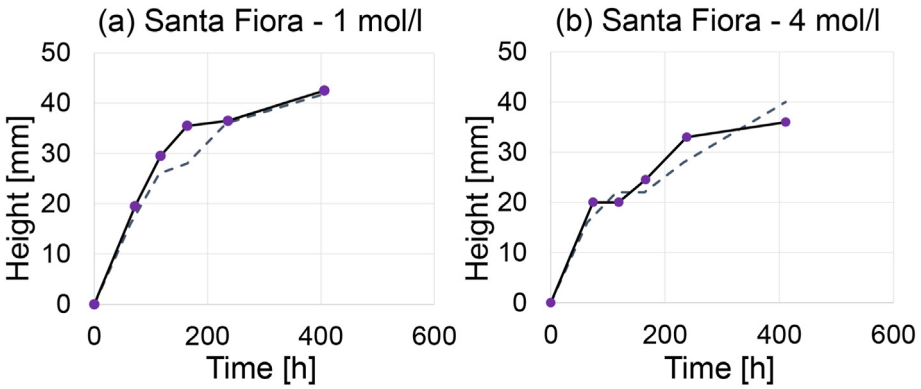

Fig. 5. Santa Fiora: Comparison of moisture penetration fronts obtained from 1D (dashed line) and 3D (solid line) measurements using (a) 1 mol/L NaCl solution and (b) 4 mol/L NaCl solution.

The acquired moisture profiles are one of the basic requirements to test the following hypothesis, in order to explain the IHRPC's significant poorer resistance to freeze and thaw with deicing salt: The moisture content in the outermost surface zone is high and decreases with respect to the penetration depth strongly. A thin moisture saturated layer forms in contact with the outer reservoir of test solution. The thin saturated layer expands during freezing. The considerable larger volume of the residual specimen shows a much lower saturation level resulting in lesser amount of expansion during freezing and hinders expansion of the thin saturated layer. This results in compressive stresses parallel to the specimen's surface, which in turn may induce considerable tensile stresses perpendicular to the surface. Because the strength of the hydrophobized concrete is lowered with respect to concrete without treatment, surface scaling is enhanced.

For each moisture state analyzed, we performed 61 1D NMR measurements with a slice thickness of approximately 3 mm and a step size of the lift of 2 mm. A coil with a diameter of 72 mm was used with a minimum echo time of 80 μs.

The concrete properties examined for both mixtures are given in Table 2. The dosage of the AEA has to be enhanced by a factor of approximately 10 for the IHRPC to obtain comparable fresh concrete properties for each mixture. This results from the negative interaction between both admixtures. In comparison to the reference mixture, the bulk density of hardened concrete as well as the compressive strength is lowered slightly. Also the spacing factor of air voids and micro air void content also decrease, which indicates a larger amount of very small air voids (10−60 μm) in the IHRPC (see Fig. 6). At larger pore sizes (60−300 μm) the number of air voids decreases with respect to the concrete without internally hydrophobic treatment, thus pore volume in this size range is slightly lower. The IHRPC absorbs significantly less moisture in total after CDF-test but shows significantly more surface scaling (see Table 2).

Moisture absorption was assessed by the integral of NMR amplitude over two defined ranges of RTD in dependence on sample depth. The following three differing states during testing were compared:

- initial state; immediate before presaturation phase starts
- presaturation state; after 168 h capillary absorption of 0.56 M (3 wt.-%) NaCl solution
- final state; after 28 freeze-thaw cycles (ftc) subsequent to the presaturation phase

Fig. 7 (a) shows the sum of NMR amplitudes corresponding to T_2-times $\geq$ 0.8 ms, which is interpreted to represent the moisture content in capillary pores. Fig. 7 (b) shows the sum of NMR amplitudes corresponding to T_2-times < 0.8 ms, which is interpreted to represent the moisture content in gel pores. The total moisture content over sample depth is shown in Fig. 7 (c). A detailed assignment of T_2-times to pore spaces of cementitious materials (white cement) is given by Fischer et al. [10]. In this study, concrete was made of grey cement with a Fe_2O_3-content of 2.97 wt.-%. It should be noted, that paramagnetic impurities generally reduce T_2-times [40].

It becomes obvious, that the IHRPC moisture profile of the capillary pores (Fig. 7 (a)) has a steeper gradient with respect to concrete without treatment, whereas the maximum total moisture content in the outermost surface is similar for both concrete types. The difference of moisture content of gel pores of both concrete types decreases with an increasing number of ftc (see Fig. 7 (b)). The gel pore moisture in the IHRPC in the initial state is higher than in the reference. Therefore, the absolute gain in gel pore moisture is higher in the reference concrete. Also it is worth noting, that the capillary moisture content in IHRPC increases slightly due to capillary suction after the presaturation phase, however, it raises considerably by subsequent alternation of freezing and thawing. The moisture transport during freezing and thawing with deicing salt is governed by micro ice lenses pump [41], cryogenic suction [42, 43, 44[42, 43, 44, e.g.] or a combination of both theories [38]. It is obviously more effective than the capillary suction, even in the IHRPC. Freezable moisture at subfreezing temperatures is located in capillary pores, where ice lenses begin to form and grow with declining temperature. The moisture in the gel pores remains unfrozen due to depression of freezing point by surface interaction. As a result of this thermodynamic disequilibrium the moisture in gel pores is squeezed out into capillary pores and freezes at the ice lenses. During thawing the hardened cement paste relaxes and gel pores absorb the moisture again. If an external moisture reservoir is available, additional moisture will be absorbed and accumulated in the hardened cement paste with every further ftc [41]. The observed moisture gradient with

Table 2
Properties of fresh as well as hardened concrete with and without internal hydrophobization. Errors represent single standard deviation.

Concrete Properties				without			with		
			limit value	Internal hydrophobization					
Fresh concrete	Time after mix begin	[min]		10	30	45	10	30	45
	Bulk density	[g/cm^3;]		2.252	2.250	2.253	2.244	2.251	2.251
	Air void content	[vol.-%]	5.5 < x < 6.5	5.6	6.0	5.7	5.9	6.0	5.6
	Degree of compactibility	[−]		1.18	1.23	1.25	1.24	1.27	1.26
Hardened concrete	Bulk density 150 mm cube (28 d)	[g/cm^3]	−	2.277 ± 0.02			2.260 ± 0.04		
	Compressive strength 150 mm cube (28 d)	[N/mm^2]	−	43.7 ± 1.4			38.1 ± 1.0		
	Spacing factor	[mm]	<0.2	0.15			0.11		
	Micro air void content A300	[vol.-%]	>1.8	2.80			2.51		
	Total moisture gain after CDF-test	[%] of specimen weight	−	1.27 ± 0.05			0.79 ± 0.04		
	Surface scaling	[g/m^2]	<1500	132 ± 27			544 ± 98		

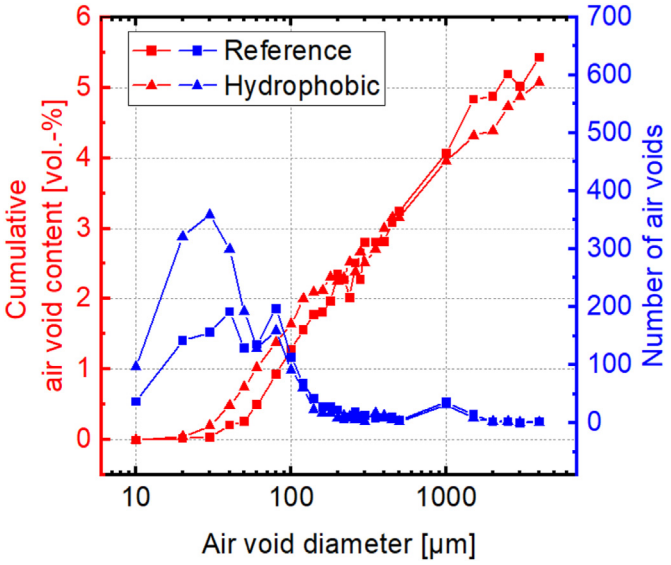

Fig. 6. Air void size distribution examined by linear-traverse method with an optical microscope.

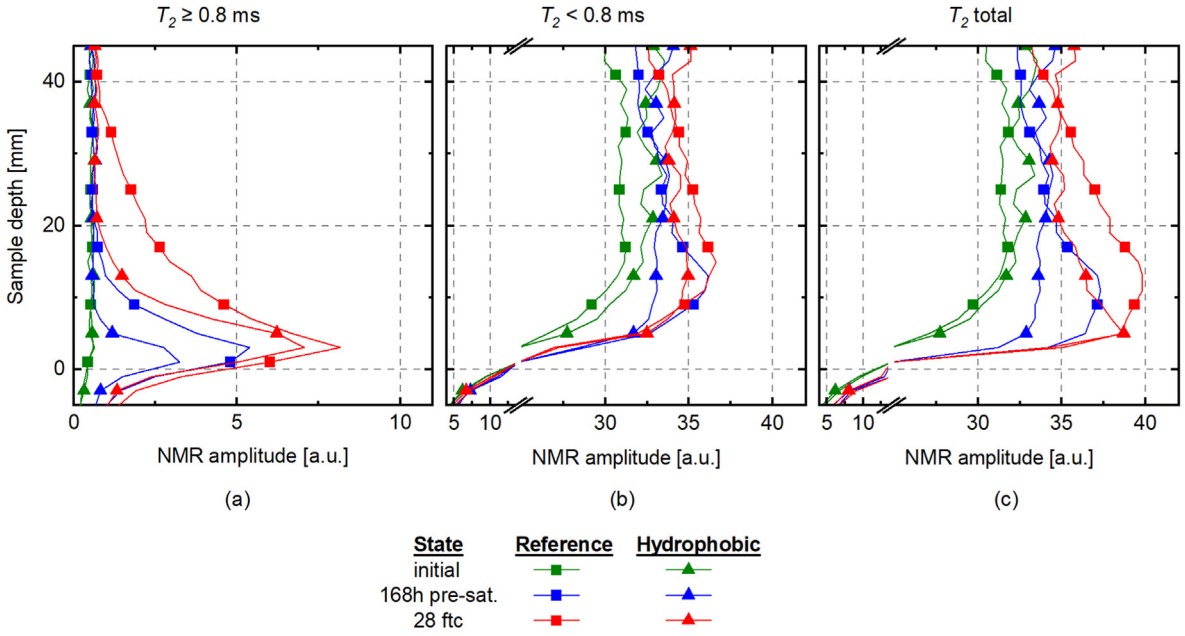

Fig. 7. Moisture profiling during presaturation and freeze-thaw cycle phase in modified CDF-test samples; (a) NMR amplitudes for T_2-times $\geq$ 0.8 ms; (b) NMR amplitudes for T_2-times < 0.8 ms; (c) NMR amplitudes for all T_2-times.

penetration depth in capillary pores in IHRPC suggests a considerable amount of freezeable moisture in a volume confined by maximum penetration depth of 15–20 mm (see Fig. 7 (a)). In the reference concrete the volume, where ice lenses are likely to form is less confined by the maximum penetration depth of approximately 40 mm (see Fig. 7 (a)). The ability to build up sufficiently high tensional stress by hindered expansion of the freezing volume to reach the concrete's tensile strength is still matter of further investigation.

2.5. Thermally-induced moisture redistribution

Concrete, in particular high-strength concrete, is prone to explosive spalling in the case of fire exposure. Currently, thermohydraulic and thermomechanical damage mechanisms are commonly considered as the main causes of explosive

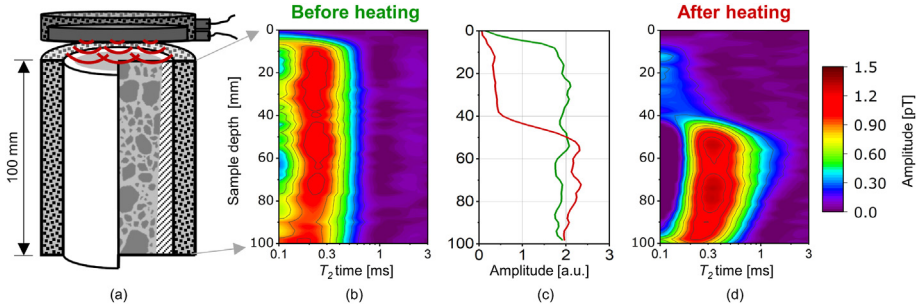

Fig. 8. (a) Schematic depiction of the miniaturized concrete specimen; (b) and (d) Heatmap of RTD before (b) and after (d) unilateral heating in dependence on the specimen's depth; (c) Total amplitude before and after unilateral heating.

spalling [45,46]. The thermomechanical damage mechanism bases on stress inhomogeneities as a result of the temperature gradient within the fire exposed component. The present contribution focuses on the thermohydraulic spalling mechanism. For this mechanism, the "moisture clog" theory plays an important role. The theory, developed by [47,48], states that as a result of thermal exposure, the water present in the concrete is released and evaporates. This leads to a pressure induced moisture flow towards the heated surface of the concrete as well as to the inner part of the heated concrete. As a result of the existing temperature gradient, the water condenses in deeper specimen areas and leads to a water-saturated zone, the so called moisture clog. This zone is impermeable for water vapor, which impedes the flow of water vapor in the specimen and can result in high pore pressures that can cause explosive spalling. To understand the thermohydraulic damage mechanisms, the knowledge of the moisture transport and reconfiguration processes within concrete during thermal exposure is of central importance.

In the last decade, different experimental investigations have been carried out to confirm the moisture clog theory. An overview of these approaches including NMR measurements are given in [13].

Based on the setup in [13], NMR measurements were carried out on miniaturized concrete specimens before and after unilateral heating. Thereby, it was the aim to improve the depth resolution as well as to reduce the echo time. The miniaturized specimen simulates a large, planar building component and requires a one-dimensional heat and moisture flux inside the concrete specimen during the thermal exposure. Therefore, the radial heat and moisture loss through the shell surface are prevented by means of a double layer shell made of glass ceramic and high-temperature wool (see Fig. 8 (a)).

The NMR measurements were performed with the 52 mm-coil and an echo time of 70 μs. In order to obtain depth-dependent results with a resolution of 2 mm, slice-selective measurements perpendicular to the heated surface of the specimen were utilized using the slice gradient system of the NMR tomograph. Each measurement consisted over 50 slice-selective measurements and took about 1.5 h.

The depth-dependent results of the NMR measurements conducted before and after heating of the specimen are shown in Fig. 8 (b)–(d). In addition to the total detectable amplitude (see Fig. 8 (c)) that corresponds to the moisture content, the distributions of the T_2-time dependent amplitude before (b) and after (d) the unilateral heating are shown.

The different relaxation times indicate different pore sizes or bonding strengths of moisture in the cement matrix. Before heating, an almost homogeneous moisture distribution across the specimen depth is visible. Most of the detectable moisture exhibits transversal relaxation times below 0.3 ms indicating moisture in gel pores [10]. After unilateral heating, the moisture content near the heated surface decreases. Behind this drying zone, a zone with higher amplitudes is visible characterized by longer T_2-times of up to 1–2 ms (see Fig. 8 (d)). This zone corresponds to a moisture accumulation, the so called moisture clog. In addition to the higher total amplitude, the change in transverse relaxation times shows that there is also a rearrangement of moisture into larger pores, for example the capillary pores [10]. This must also be considered in connection with a thermally induced pore structure change due to the decomposition of the hardened cement paste phases [49].

3. Summary and conclusion

^{1}H NMR relaxometry is a relatively new and powerful analytical technique that is gaining popularity in the study of building materials. It has been used as a non-destructive tool to analyze the physical and chemical properties of materials, such as their water content, porosity, and hydration mechanisms. In this paper, we present the functionality of the NMR core analyzing tomograph which was custom built to meet our requirements for the investigation of both any moisture related damage processes as well as the characterization of alternative, more climate friendly (more heterogeneous in composition) building materials.

The new device proved to be a very sensitive tool for even very small changes in absolute moisture content (down to 0.03 g) and the spatial moisture distribution. Even after oven-drying at 70 °C and 105 °C degrees a residual moisture content was measurable in sandstones. Hence, for better comparability with other methods, the NMR signal needs to be calibrated.

The small echo times and the variable coil diameters allow the detection of highly bound water (e.g., in gel pores of cement-bound building materials) with high SNR. By using slice-selective measurements the moisture content as well as the

RTD can be determined with a depth resolution of up to 1–4 mm. We could show that moisture changes (e.g., due to different exposures such high temperatures, freeze thaw, capillary suction) can be determined and quantified.

Depending on the pore size distribution of the materials, it is also possible to study the ingress of moisture in 3D. However, this is mainly successful when larger pores or cracks prevail which are characterized by higher echo times ($\geq$ 1.8 ms).

With the NMR tomograph, we have further succeeded in performing automated measurements on larger and heterogeneous, cementitious samples with many echoes and short echo intervals over a period of several days to monitor the hydration. This had previously only been demonstrated on much smaller samples with about 1/5 of the volume and, in our opinion, opens up a unique opportunity for further the characterization of climate-sensitive binders with heterogeneous additives.

CRediT authorship contribution statement

Sabine Kruschwitz: Conceptualization of subsections 2.1, 2.2, 2.3, Data Curation, Validation; Visualization, Writing - Original draft preparation, Writing - review & editing, Supervision. **Sarah Munsch:** Conceptualization of subsection 2.1, Data curation, Validation, Visualization, Writing - original draft preparation, Writing - review & editing. **Melissa Telong:** Data curation, Validation; Visualization, Writing - review & editing. **Wolfram Schmidt:** Conceptualization of subsection 2.2, Validation, Visualization, Writing - original draft preparation, Writing - review & editing. **Thilo Bintz:** Conceptualization of subsection 2.3, Data curation, Validation, Visualization, Writing - original draft preparation, Writing - review & editing. **Matthias Fladt:** Conceptualization of subsection 2.4, Data curation, Validation, Visualization, Writing - original draft preparation, Writing - review & editing. **Ludwig Stelzner:** Conceptualization of subsection 2.5, Data curation, Validation, Visualization, Writing - original draft preparation, Writing - review & editing.

Declaration of competing interest

The authors declare that they have no known competing financial interests or personal relationships that could have appeared to influence the work reported in this paper.

Acknowledgements

We would like to thank Marco Lange from the technical staff at BAM who provided valuable assistance with the sample preparation for the studies in Chap. 2.1 and 2.3. We would like to extend our appreciation to the concrete lab and our colleague Frank Haamkens in particular for his support with casting of the materials. Their expertise and support made a significant contribution to the success of our project. We thank Dr. Frank Weise for initiating the research on internal hydophobisation and fire exposure of concretes at BAM and providing scientific support for the research presented in Chap. 2.4 and 2.5.

References

[1] G.R. Coates, L. Xiao, M.G. Prammer, NMR Logging — Principles and Applications, Halliburton Energy Services, Houston, 1999.
[2] K.-J. Dunn, D.J. Bergman, G.A. Latorraca, Nuclear Magnetic Resonance - Petrophysical and Logging Applications, Volume 32 of *Handbook Of Geophysical Exploration*, Elsevier, Oxford, 2002.
[3] R. Kimmich, NMR Tomography Diffusometry Relaxometry, Springer Berlin Heidelberg, 1997, https://doi.org/10.1007/978-3-642-60582-6.
[4] B. Blümich, S. Haber-Pohlmeier, W. Zia, Compact NMR, De Gruyter, Berlin, 2014, https://doi.org/10.1515/9783110266719.
[5] C. Rehorn, B. Blümich, Cultural heritage studies with mobile NMR, Angew. Chem. Int. Ed. 57 (2018) 7304–7312.
[6] C. Nunes, L. Pel, J. Kunecký, Z. Slížková, The influence of the pore structure on the moisture transport in lime plaster-brick systems as studied by NMR, Construct. Build. Mater. 142 (2017) 395–409.
[7] H. Liu, M.N. d'Eurydice, S. Obruchkov, P. Galvosas, Determining pore length scales and pore surface relaxivity of rock cores by internal magnetic fields modulation at 2 MHz NMR, J. Magn. Reson. 246 (2014) 110–118.
[8] S. Kruschwitz, M. Halisch, R. Dlugosch, C. Prinz, Toward a better understanding of low-frequency electrical relaxation — an enhanced pore space characterization, Geophysics 85 (2020) MR257–MR270.
[9] A.C.A. Muller, K.L. Scrivener, A.M. Gajewicz, P.J. McDonald, Densification of c-S-H measured by h NMR relaxometry, J. Phys. Chem. C 117 (2012) 403–412.
[10] N. Fischer, R. Haerdtl, P. McDonald, Observation of the redistribution of nanoscale water filled porosity in cement based materials during wetting, Cement Concr. Res. 68 (2015) 148–155.
[11] C. Naber, F. Kleiner, F. Becker, L. Nguyen-Tuan, C. Rößler, M.A. Etzold, J. Neubauer, C-S-H pore size characterization via a combined nuclear magnetic resonance (NMR)–scanning electron microscopy (SEM) surface relaxivity calibration, Materials 13 (2020) 1779.
[12] D.E. Woessner, The early days of NMR in the Southwest, Concepts Magn. Reson. 13 (2001) 77–102.
[13] L. Stelzner, B. Powierza, T. Oesch, R. Dlugosch, F. Weise, Thermally-induced moisture transport in high-performance concrete studied by x-ray-ct and 1h-nmr, Construct. Build. Mater. 224 (2019) 600–609.
[14] B. Min, C. Sondergeld, C. Rai, Investigation of high frequency 1D NMR to characterize reservoir rocks, J. Petrol. Sci. Eng. 176 (2019) 653–660.
[15] T. Bintz, S.M. Nagel, L. Stelzner, R. Lauinger, W. Schmidt, S. Kruschwitz, An nmr tomograph for building materials - applications, experimental studies and limitations, in: Proceedings of the 13th Conference on Electromagnetic Wave Inetraction with Water and Moist Substances, ISEMA), 2021, pp. 1–5.
[16] Pure Devices GmbH, MR-CAT, Core Analyzing Tomograph, 2022. April 2022, https://www.pure-devices.com/index.php/products/products-mr-cat.html.
[17] T. Hiller, Thohiller/nmr-nucleus: v0.1.13, 2022, https://doi.org/10.5281/zenodo.4022195 (version v0.1.13).
[18] D. Capitani, V.D. Tullio, N. Proietti, Nuclear magnetic resonance to characterize and monitor cultural heritage, Prog. Nucl. Magn. Reson. Spectrosc. 64 (2012) 29–69.

[19] J. Orlowsky, F. Braun, M. Groh, The influence of 30 Years outdoor weathering on the durability of hydrophobic agents, Appl. Obernkirchener Sandstones Build. 10 (2020) 18.
[20] M.W. Bligh, M.N. d'Eurydice, R.R. Lloyd, C.H. Arns, T.D. Waite, Investigation of early hydration dynamics and microstructural development in ordinary Portland cement using ^{1}H NMR relaxometry and isothermal calorimetry, Cement Concr. Res. 83 (2016) 131–139.
[21] DIN EN 13755:2008-08, Natural Stone Test Methods – Determination of Water Absorption at Atmospheric Pressure (German Version), Beuth Verlag, Berlin), 2008.
[22] D. Ectors, F. Goetz-Neunhoeffer, W.-D. Hergeth, U. Dietrich, J. Neubauer, In situ 1H-TD-NMR: quantification and microstructure development during the early hydration of alite and OPC, Cement Concr. Res. 79 (2016) 366–372.
[23] D. Jansen, C. Naber, D. Ectors, Z. Lu, X.-M. Kong, F. Goetz-Neunhoeffer, J. Neubauer, The early hydration of OPC investigated by in-situ XRD, heat flow calorimetry, pore water analysis and 1H NMR: learning about adsorbed ions from a complete mass balance approach, Cement Concr. Res. 109 (2018) 230–242.
[24] J. Arnold, Mobile NMR for Rock Porosity and Permeability, Ph.D. thesis, RWTH Aachen University, 2007.
[25] S. Miller, P. Cunningham, J. Harvey, Rice-based ash in concrete: a review of past work and potential environmental sustainability, Resour. Conserv. Recycl. 146 (2019) 416–430.
[26] N.S. Msinjili, W. Schmidt, A. Rogge, H.-C. Kühne, Rice husk ash as a sustainable supplementary cementitious material for improved concrete properties, Af. J. Sci. Technol. Innovat. Develop. 11 (2018) 1–9.
[27] K. Scrivener, A. Nonat, Hydration of cementitious materials, present and future, Cement Concr. Res. 41 (2011) 651–665.
[28] T. Oesch, F. Weise, D. Meinel, C. Gollwitzer, Quantitative in-situ analysis of water transport in concrete completed using x-ray computed tomography, Transport Porous Media 127 (2018) 371–389.
[29] A. Molkenthin, Laser-induzierte Breakdown Spektroskopie (LIBS) zur hochauflösenden Analyse der Ionenverteilung in zementgebundenen Feststoffen, BAM-Dissertationsreihe, 1 ed., Bundesanstalt f. Materialforschung und -prüfung, 2009.
[30] Deutscher Ausschuss für Stahlbeton, Prüfung von Beton, Empfehlung und Hinweise als Ergänzung zu DIN 1048, 1991. Beuth Verlag (Berlin).
[31] S. Millar, S. Kruschwitz, G. Wilsch, Determination of total chloride content in cement pastes with laser-induced breakdown spectroscopy (LIBS), Cement Concr. Res. 117 (2019) 16–22.
[32] J.J.O. Andrade, E. Possan, D.C.C.D. Molin, Considerations about the service life prediction of reinforced concrete structures inserted in chloride environments, J. Build. Pathol. Rehabilit. 2 (2017).
[33] A. Miziolek, V. Palleschi, I. Schechter, Laser Induced Breakdown Spectroscopy, 2006.
[34] F. Weise, M. Fladt, M. Wieland, Internal water-repellent treatment—a novel strategy for mitigating alkali-aggregate reaction in concrete pavements, in: Proceedings of the 16th International Conference on Alkali-Aggregate Reaction in Concrete, vol. 1, 2021, pp. 511–524.
[35] M.J. Setzer, G. Fagerlund, D.J. Janssen, CDF test—test method for the freeze-thaw resistance of concrete-tests with sodium chloride solution (CDF), Mater. Struct. 29 (1996) 523–528.
[36] G.G. Litvan, Frost action in cement paste, Matériaux et construction 6 (1973) 293–298.
[37] M.J. Setzer, Frostschaden grundlagen und prüfung, Beton-und Stahlbetonbau 97 (2002) 350–359.
[38] M. Müller, H.-M. Ludwig, M.T. Hasholt, Salt frost attack on concrete: the combined effect of cryogenic suction and chloride binding on ice formation, Mater. Struct. 54 (2021) 1–16.
[39] T.C. Powers, R. Helmuth, Theory of volume changes in hardened portland-cement paste during freezing, in: Highway research board proceedings 32, 1953.
[40] R. Schulte Holthausen, M. Raupach, in: h.-m Ludwig (Ed.), Determination of Porosity and Pore Size Distribution in Concrete by Singlesided ^{1}H NMR—From White Cement Pastes to Grey Cement Mortars, 2018. IBAUSILWeimar.
[41] M. Setzer, The micro ice lens pump—a new sight of frost attack and frost testing, in: N. Banthia, k. Sakai, O.E. Gjřrv (Eds.), Proceedings Third International Conference on Concrete under Severe Conditions, The University of British Columbia, Canada, Vancouver, 2001, pp. 428–438.
[42] S. Lindmark, Mechanisms of Salt Frost Scaling of Portland Cement-Bound Materials: Studies and Hypothesis, Ph.D. thesis, Lund University, 1999.
[43] C. Borgnakke, W. Hansen, Y. Kang, Z. Liu, E. Koenders, Cryogenic suction pump mechanism for combined salt-and frost exposure, in: G. Ye, K. van Breugel, W. Sun, C. Miao (Eds.), RILEM Proceedings Pro083 : Microstructural-Related Durability of Cementitious Composites, Second International Conference on Microstructural-Related Durability of Cementitious Composites, RILEM Publications S.A.R.L., France, 2012, pp. 1–8. Cd paper 185; Second international conference on microstructural-related durability of cementitious composites, Amsterdam, The Netherlands ; Conference date: 11-04-2012 Through 13-04-2012.
[44] Z. Liu, W. Hansen, A hypothesis for salt frost scaling in cementitious materials, J. Adv. Concr. Technol. 13 (2015) 403–414.
[45] R. Jansson, L. Boström, Fire spalling: theories and experiments, in: Proceedings of the Fifth International RILEM Symposium on Self-Compacting Concrete, Ghent, 2007, pp. 735–740.
[46] P. Kalifa, F.-D. Menneteau, D. Quenard, Spalling and pore pressure in hpc at high temperatures, Cement Concr. Res. 30 (2000) 1915–1927.
[47] G.W. Shorter, Harmathy, Discussion on the fire-resistance of prestressed concrete beams, Proceed. Institut. Civil Eng. 17 (1960) 15–38.
[48] T.Z. Harmathy, Effect of Moisture on the Fire Endurance of Building Elements, vol. 385, ASTM Special Technical Publication, 1965, pp. 74–95.
[49] G.-F. Peng, Z.-S. Huang, Change in microstructure of hardened cement paste subjected to elevated temperatures, Construct. Build. Mater. 22 (2008) 593–599.

Sabine Kruschwitz obtained a Master's degree in Geophysics from the Technical University of Berlin (TUB) in 2002, and has since worked on numerous national and international research projects at the Bundesanstalt für Materialforschung und -prüfung (BAM). She completed her PhD at TUB in 2007 and has gained additional expertise during both of her one year stays at NIST and the Rutgers University, USA. In 2016, Sabine was appointed as Junior Professor, heading the “Nondestructive Building Material Testing” division at TUB. Concurrently, she leads a junior research group at BAM with a focus on “Material Characterization and Informatics for the Sustainability in Civil Engineering”.

Sarah Munsch obtained her Master's degree in Geotechnology at the Technische Universität Berlin in 2017. Since then she works as a scientific assistant at Bundesanstalt für Materialforschung und -prüfung. Her work is mainly focused on the conduction and evaluation of NMR measurements on various porous building materials with respect on moisture ingression profiles, porosity determination and pore space characterization. A doctoral thesis about the interpretation of NMR signals in partly saturated sandstones is in progress. E-mail: sarah.munsch@bam.de

Melissa Telong obtained her Master's degree in Civil Engineering at the Technische Universität Berlin in 2022. Subsequently she started working as a scientific assistant at Bundesanstalt für Materialforschung und -prüfung, where she mainly uses NMR to characterize the hydration behavior of fresh mortar and concrete samples and the pore space characteristics of hardened samples. She is also investigating ways to predict, e.g. carbonation behavior based on NMR results using AI methods. E-mail: melissa.telong@bam.de

Wolfram Schmidt works at in the department “Safety of Structures” at BAM, responsible for the rheology and admixtures laboratory with a research focus on innovative cement and concrete constituents. Furthermore, he is secretary of the German Rheological Society, founder of the Pan-African cement round robin (PACE-PTS) and initiator of the conference series “Advances in Cement and Concrete Technology in Africa” (ACCTA) and ISEE-Africa (Innovation, Science, Engineering, Education). He received the German-African Innovation Incentive Award and is member of RILEM and fib and among others convenor for sub-Saharan Africa and officer in the RILEM Development Advisory Committee.

Thilo Bintz studied Geology at Freie Universität Berlin and earned a Master's degree in Geophysics. He has worked as a research assistant at the Technische Universität Berlin and the Bundesanstalt für Materialforschung und -prüfung, where he is currently pursuing a PhD focusing on the transport of moisture and deleterious ions in building materials. For his studies Thilo uses NMR and LIBS investigating transport processes of mostly alternative and more environmentally friendly types of cementitous binders. E-mail: thilo.bintz@bam.de

Matthias Fladt completed his Master's degree in Geosciences at Heidelberg University in 2017. After a five-month internship at Heidelberg Materials he joined the Bundesanstalt für Materialforschung und -prüfung as a research assistant in 2018. His research focus is on evaluating the effectiveness of internal hydrophobic treatment of road pavement concrete in preventing alkali-silica reaction. Additionally, he is studying the impact of hydrophobic treatment on moisture ingress, particularly after a freeze-thaw cyclic exposure. E-mail: matthias.fladt@bam.de

Ludwig Stelzner received his doctoral degree in civil engineering from Institute of Construction Materials, University of Stuttgart in Germany in 2021. He is currently working as a postdoc at the department of Fire Engineering at the Bundesanstalt für Materialforschung und -prüfung in Berlin. His research field is material and structural behavior of concrete during fire exposure. E-mail: ludwig.stelzner@bam.de